PHYSICAL REVIEW B **81**, 060402(R) (2010)

Domain-wall spin-torque resonators for frequency-selective operation

S. Lepadatu,[1,*] O. Wessely,[2,3] A. Vanhaverbeke,[4] R. Allenspach,[4] A. Potenza,[5] H. Marchetto,[5,6] T. R. Charlton,[7] S. Langridge,[7] S. S. Dhesi,[5] and C. H. Marrows[1,†]

[1]*School of Physics and Astronomy, E.C. Stoner Laboratory, University of Leeds, Leeds LS2 9JT, United Kingdom*

[2]*Department of Mathematics, Imperial College, London SW7 2BZ, United Kingdom*

[3]*Department of Mathematics, City University, London EC1V 0HB, United Kingdom*

[4]*IBM Research, Zurich Research Laboratory, CH-8803 Rüschlikon, Switzerland*

[5]*Diamond Light Source, Chilton, Didcot OX11 0DE, United Kingdom*

[6]*Fritz-Haber-Institute der Max-Planck-Gesellschaft, Faradayweg 4-6, 14195 Berlin, Germany*

[7]*ISIS, STFC Rutherford Appleton Laboratory, Chilton, Didcot OX11 0QX, United Kingdom*

(Received 19 November 2009; published 4 February 2010)

In this work we demonstrate control of the spin-torque resonance frequency of a domain wall (DW) in a notched wire through the lithographic engineering of the shape and profile of the notch. By modeling the magnetization dynamics of a current-driven domain wall in a nanometric constrained geometry, an almost harmonic pinning potential has been designed, and we experimentally demonstrate the operation of domain wall resonators with well-defined, selectable resonance frequencies, suitable for application in zero magnetic field. These results show that the DW may be treated to a good approximation as a quasiparticle acted on by a restoring force that may be derived from the notch shape in a physically transparent manner.

DOI: 10.1103/PhysRevB.81.060402 PACS number(s): 75.60.Ch, 72.25.Pn, 72.25.Ba

Using spin-transfer torque[1,2] to manipulate domain walls in nanoscale magnetic elements has potential applications in spintronic devices[3] for memory[4] or logic.[5] The spin-torque resonance effect[6,7] allows for a domain wall to be excited using an alternating current that is tuned to the eigenfrequency of a potential well. A pinning potential for a domain wall (DW) in a magnetic nanowire generally arises when a geometric deformation, such as a notch, is introduced, giving rise to a variation of the total energy of the system with the position of the DW. The gradient of the total energy along the pinning potential can be interpreted as a restoring force acting on the DW,[8] naturally bringing the DW to the minimum energy position. Such pinning sites not only allow for the interaction between a DW and spin-polarized current[9–11] to be studied, but are important for device applications, for instance magnetic memory devices where binary data may be stored as the presence or absence of a DW in such a pinning potential. Using the effect of spin torque resonance allows for the DW to be depinned at much lower threshold currents when the frequency of the excitation current is tuned to the eigenfrequency of the pinning potential.[7,12–14]

The structures investigated here consist of 20-nm-thick permalloy ($Ni_{80}Fe_{20}$) with a 1.5 nm Al capping layer, obtained by liftoff following electron-beam lithography and sputtering of the NiFe/Al bilayer. The geometry consists of a magnetic wire with a central geometric constriction and an elliptical DW nucleation pad at one end, as shown by the scanning electron microscopy (SEM) image in Fig. 1(a). The pinning potentials investigated here are defined by linear and parabolic notches of variable steepness. The wire width and constriction width were kept fixed at 1 μm and 100 nm respectively, while the profile of the notch was varied, as summarized in Table I. DWs were nucleated in the pad and propagated to the center of the notches by applying a sequence of magnetic fields, as described previously[9,10]

The structure of the DWs pinned at the notches was investigated by means of x-ray magnetic circular dichroism (XMCD) combined with PEEM imaging[15] and scanning electron microscopy with polarization analysis (spin-SEM).[16] PEEM imaging was carried out at the I06 beamline at the Diamond Light Source synchrotron, using circularly polarized x-ray photons with energies corresponding to the Fe L_3 and L_2 absorption edges, while spin-SEM imaging was carried out at IBM Zurich Research Laboratory. All magnetic imaging was carried out at near-zero magnetic field (less than 1 Oe). Our wires are of a size where vortex DWs are to be expected in the main parts, and transverse DWs at the narrowest part of the notch.[17] Figure 1(b) shows a spin-SEM image of a wire with a parabolic notch. Here the elliptical pad contains a complex domain structure, formed in the DW creation process, while the wall is pinned in the center of the notch. Figures 1(c) and 1(d) show PEEM images of DWs pinned in linear notches of different angle. For the notch in Fig. 1(d) one can also see that a DW is pinned at the center of the constriction, while in Fig. 1(c), where the notch angle is steeper, a complex vortexlike DW has failed to fully enter the notch.

To allow for electrical measurement, 10 nm Ta/140 nm Au leads were attached to the wires, centered around the notches in a two-point measurement configuration. The frequency variation of the sample resistance was measured in reflection mode using a high frequency measurement setup based on a vector network analyzer. For each frequency value a sinusoidal voltage of fixed amplitude is applied to the sample for 1 s and the reflected voltage is measured to obtain the real and imaginary parts of the voltage reflection coefficient, or S_{11} parameter. Using a transmission line of characteristic impedance of 50 Ω the sample resistance is obtained from the magnitude of the S_{11} voltage reflection coefficient parameter. This is justified since the resonance appears only in the real part of S_{11}, showing that the resonance peak appears due to a change in sample resistance only. Typical frequency scans are shown in Fig. 1(e), measured at zero magnetic field for the states with and without a pinned DW at the constriction

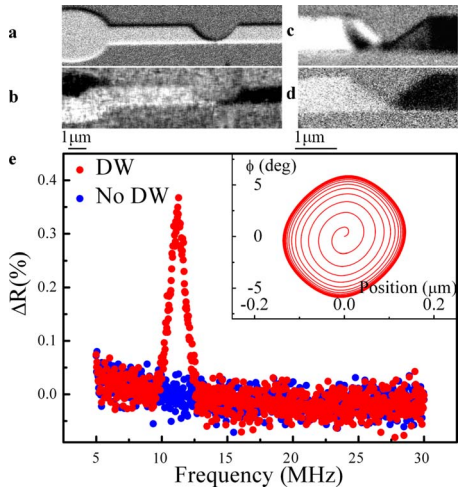

FIG. 1. (Color online) (a) SEM image of a typical structure, in this case with a parabolic (P2) pinning site, (b) spin-SEM image showing the equilibrium pinning position of a DW in the parabolic notch P2. PEEM images showing the equilibrium pinning position of a DW in the linear notches (c) L4 and (d) L3. The magnetization component along the length of the wire is given as a gray scale contrast in (b) to (d), with opposite orientation coded as black and white. (e) Resistance change as a function of frequency for a linear pinning potential, L1, in the states with and without a pinned DW, where the current density was fixed at 2.6×10^{11} A/m^2. The inset shows the calculated DW oscillation dynamics, starting from the initial state at rest, and reaching a steady periodic orbit in $q-\phi$ space. Sample identification numbers are explained in Table I.

and using a sinusoidal voltage of fixed amplitude, corresponding to a peak current density of 2.6×10^{11} A/m^2 at the narrowest part of the constriction. For the state without a DW the resistance is found to be quite featureless with frequency, while for the state with a pinned DW, a pronounced peak in the measured resistance is observed. For the case of the frequency response shown in Fig. 1(e), the measured resistance peak observed for the state with a pinned DW is expected to arise due to the coherent DW oscillation at the resonance frequency, resulting in enhanced energy dissipation, and thus an increase in the measured resistance.

We now develop a model for the DW motion excited by a spin polarized current, similar to the one-dimensional (1D) model of Malozemoff and Slonczewski.[18] For a magnetic wire with position and time dependent magnetization density $\boldsymbol{M}=M_s[\cos(\theta),\sin(\theta)\cos(\phi),\sin(\theta)\sin(\phi)]$, the dynamics of the magnetization are given by the Lagrangian

$$L=-\int\frac{M_S}{\gamma}(\cos\theta-1)\dot{\phi}dV-E \qquad (1)$$

where the integral is over the volume of the wire and E is the total energy. The magnetization lies at an angle θ, in the $x-y$ plane which contains the wire, to the wire axis (the DW lying between domains where $\theta=0$ or π), and points out of that plane by an angle ϕ. For a narrow magnetic strip elongated in the x direction, the magnetostatic energy is approximately given by an easy axis and an easy plane anisotropy energy, K_0 and K, respectively, which can be estimated from

TABLE I. Summary of the various pinning potentials investigated, giving the values of g and c, the parameters which define the steepness of the linear and parabolic notches, for each nanowire sample. These parameters enter the relationship between the width of the wire y with position along the wire, x .

Linear pinning potentials: $y=g\|x\|$					
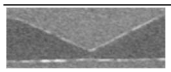	L1	L2	L3	L4	L5
g	0.36	0.45	0.6	0.9	1.8
Parabolic pinning potentials: $y=cx^2$					
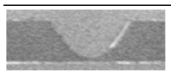	P1	P2	P3	P4	P5
$c/10^6$	0.5	0.73	0.91	1.49	3.25

the corresponding quantities of an infinitely long ellipsoid.[14,19] By also assuming that the magnetization is approximately uniform in the y (across the strip) and z (normal to the strip) directions the following expression for the total energy is obtained

$$E=\int\left\{A\left[\left(\frac{\partial\theta}{\partial x}\right)^2+\sin^2\theta\left(\frac{\partial\phi}{\partial x}\right)^2\right]-(K_0\cos^2\theta-K\sin^2\theta\sin^2\phi)\right\}S(x)dx \qquad (2)$$

where $S(x)$ is the cross sectional area of the wire perpendicular to the x direction, and A is the exchange stiffness constant. The 1D approximation assumes that the DW is transverse with $\phi=\phi(t)$ and $\theta=2\tan^{-1}(\exp\{[x-q(t)]/\Delta\})$, where q is the position of the DW and Δ is the DW width.[18] The magnetostatic energy increases for a tilted DW, and the increase causes the DW to contract, hence we further assume that the DW width Δ is given by $\Delta(\phi)=\Delta_0/(1+(K/K_0)\sin^2\phi)^{1/2}$. where the static DW width $\Delta_0=\Delta(0)=(A/K_0)^{1/2}$. Our formulation differs from the one by Tatara *et al.* where the DW width is considered to be a constant,[20] and the one by Thiaville *et al.* where the DW width is treated as an independent parameter.[21] Usually the pinning potential in the 1D model is assumed to take an arbitrary form where its depth and width are indirectly obtained from experiments and micromagnetic simulations.[7,12,14] To take account of the shape of the different pinning profiles used in the experiment we instead derive an explicit expression for the pinning potential given by the experimental notch geometry and materials properties: there are no adjustable fitting parameters. The expression is obtained by considering the fact that for a transverse DW the total DW energy E is, to a good approximation, proportional to the cross-sectional area of the wire at the position of the DW,[22] where the energy per unit area is $4A/\Delta$. The pinning potential will thus depend on both q and ϕ since the cross section area depends on q, and the DW tends to contract as its magnetization tilts. If the magnetization profile of the transverse DW is inserted in Eqs. (1) and (2) the following q and ϕ dependent Lagrangian is obtained:

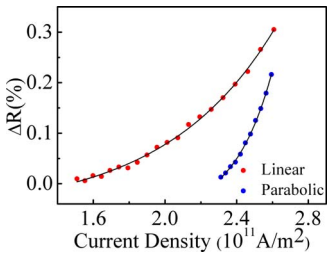

FIG. 2. (Color online) Variation of resonance peak height with current density for linear (L1) and parabolic pinning potentials (P1). Solid lines are guides to the eyes.

$$L = -\int \frac{M_S}{\gamma}\left[\tanh\left(\frac{x-q}{\Delta(\phi)}\right) - 1\right]\dot{\phi}S(x)dx - E, \tag{3}$$

$$E = \frac{4A}{\Delta(\phi)}\int \frac{1}{2\Delta(\phi)\cosh^2((x-q)/\Delta(\phi))}S(x)dx. \tag{4}$$

For a wire where $S(x)$ is slowly varying compared to $\{2\Delta\cosh^2[(x-q)/\Delta]\}^{-1}$ the Lagrange equation of motion for q and ϕ takes the form

$$\dot{q}S(q) = -\frac{\gamma}{2M_S}[2\Delta K\sin(2\phi)S(q)], \tag{5}$$

$$\dot{\phi}S(q) = \frac{\gamma}{2M_S}\left[\frac{4A}{\Delta}\int_{-\infty}^{\infty}\frac{S'(x)}{2\Delta\cosh^2((x-q)/\Delta)}dx\right] \tag{6}$$

where the terms in square bracket in Eq. (5) and (6) are $\partial E/\partial\phi$ and $\partial E/\partial q$, respectively.

If the current induced spin transfer torque and Gilbert damping are included in the two coordinate model[20,21,23] the equations of motion for q and ϕ take the form

$$(\dot{q} - \alpha\Delta\dot{\phi})S(q) = -\frac{\gamma}{2M_S}\frac{\partial E}{\partial\phi} + \frac{J(q)\mu_B P}{eM_S}S(q), \tag{7}$$

$$\left(\dot{\phi} + \frac{\alpha}{\Delta}\dot{q}\right)S(q) = \frac{\gamma}{2M_S}\frac{\partial E}{\partial q} \tag{8}$$

where $J(q)$ is the current density at the position of the DW, $S(q)$ is the position-dependent cross-sectional area of the wire, P is the spin polarization of the current, M_s is the saturation magnetization, α is the Gilbert damping constant and e, μ_B and γ are electron charge, Bohr magneton and gyromagnetic ratio respectively. The solution to the above equations for a given current density is a trajectory in (q and ϕ) space [see inset to Fig. 1(e)]. After some transient motion the trajectory eventually settles to a steady orbit from which the oscillation frequency can be extracted.

Looking first at the linear pinning potentials, which have been previously much studied,[9,10,24,25] the DW resonance mechanism is investigated as a function of current density. The resonance peak height is found to depend monotonically on current density as shown in Fig. 2, increasing once a threshold value of current density is exceeded. This general qualitative dependence of the peak height on current density is found to hold for the linear pinning potentials L1 through to L3. On the other hand for the pinning potentials L4 and L5 no resonance peaks have been observed: in the PEEM images we observed that these are the two cases where the DW does not fully enter the notch.

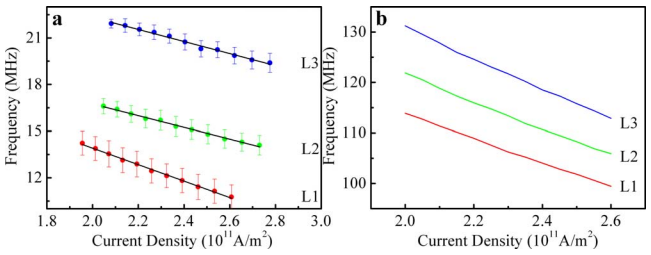

FIG. 3. (Color online) Resonance frequency as a function of current density for the linear pinning potentials L1 through to L3, showing (a) experimental results with FWHM error bars and (b) theoretical results. In the theoretical calculation the ratio between the easy plane and easy axis anisotropy $(K/K_0)=6$ and the static DW width $\Delta_0=70$ nm, based on the geometry of the linear notches.

For the linear pinning potentials the dependence of the center frequency of the resonance peak on the current density is shown in Fig. 3(a), where the error bars represent the full width at half maximum (FWHM) of the resonance peaks. For a fixed current density the resonance frequencies can be controlled by changing the notch profile. As the constriction, and hence pinning potential, becomes steeper, the effective restoring force acting on the DW rises, leading to higher resonance frequencies. On the other hand, the resonance frequency is found to depend strongly on the current density for the pinning potentials L1 through to L3, with overlapping frequency domains. Thus the DW oscillation cannot be described by a simple harmonic oscillator with a fixed resonance frequency. This is due to the highly anharmonic potential, e.g., there is a discontinuity in restoring force at the origin.

As shown in Fig. 3(b), for the linear pinning potentials, the qualitative agreement between the measured and calculated frequencies is excellent. In particular both the measured and calculated resonance frequencies change by around 14% over a range of 6×10^{10} A/m^2 compared to the respective values obtained at 2×10^{11} A/m^2. However due to the simplified shape of the DW used in the theory, the model predicts a higher frequency than the experimentally observed one. The easy plane and the easy axis anisotropy in general depend on the dimensions of the wire cross section, and thus vary with the position of the DW. In this work we neglected this q dependence, and consider K_0 and K to be average values of the corresponding quantities. Furthermore the shape of a DW moving in a magnetic wire is known to deviate from the form assumed in the 1D model. It is for example known that for very large tilt angles ϕ. an antivortex will be formed at the edge of the wire which tends to drastically slow down the motion of the DW.[26] It is thus not surprising that our theoretical resonance frequency is higher than the experimental one. A fully micromagnetic model should be able to address this issue, at the loss of some physical transparency. For permalloy we have used the standard parameters of the saturation magnetization $M_s=8.7\times10^5$ A/m, the exchange stiffness constant

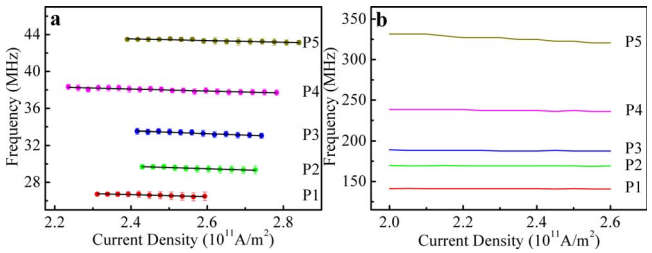

FIG. 4. (Color online) Resonance frequency as a function of current density for the parabolic pinning potentials P1 through to P5, showing (a) experimental results with FWHM error bars and (b) theoretical results. In the theoretical calculation the ratio between the easy plane and easy axis anisotropy $(K/K_o)=6$ and the static DW width $\Delta_0=40$ nm. The DW width is lower than the corresponding value for the linear notches since the average constriction width is smaller for the parabolic notches.

$A=1.3\times10^{-11}$ J/m, the damping $\alpha=0.01$ (Ref. 27) and the spin polarization of the current $P=0.4$.[9] Nonadiabatic torque can also be incorporated in the 1D model,[12,20,23] but we have found that its effect is negligible for the applications considered in this Rapid Communication. Even though we do not obtain a quantitative agreement between experiment and theory, the good qualitative agreement shows that the model captures the essentials of the physics with some fairly simple and obvious assumptions, and that to a certain extent the DW may be treated as a quasiparticle in a potential defined in a fairly physically transparent way by the shape of the notch.

The nonharmonic behavior of a DW oscillating in a linear notch can be explained by considering the right-hand side of Eq. (7). The restoring force $\partial E/\partial q$ is determined by the spatial derivative of the cross sectional area, S', which for a linear notch is not proportional to the DW displacement from equilibrium. We therefore went on to design, fabricate, and study nanowires with parabolic notches (samples P1-P5) where S' is proportional to the DW displacement, which we expect to be more harmonic. Spin-SEM imaging showed DWs at the center of all five notches, and we observed resonance peaks for all five samples. Once again, the resonance peak height increases with current density once a threshold value is exceeded, as shown in Fig. 2. The experimental results for the resonance frequencies of the parabolic pinning potentials P1 to P5 are shown in Fig. 4(a), where the resonance frequency is plotted as a function of current density. As for the linear potentials, the resonance frequency increases as the pinning potential profile becomes steeper, but here we observed well-defined eigenfrequencies for each notch. Once again the qualitative agreement with theory is good: the calculated oscillation frequencies were found to be almost independent of the driving current, as shown in Fig. 4(b). In particular both the measured and calculated resonance frequencies change by around 1% over a range of 6×10^{10} A/m^2 compared to the respective values obtained at 2×10^{11} A/m^2. By engineering the shape of the notch using lithographic techniques we show that the current driven DW resonance may be controlled and set to be nearly independent of the driving force. We also show that the DW resonance may be sustained without the use of applied magnetic fields, with the restoring force on the DW being derived from the geometric pinning potential alone.

Moreover, the Q factors of the resonances, defined as the center frequency divided by the FWHM (the latter shown as error bars in Figs. 3 and 4), are much larger for the parabolic notches. For the linear potentials we have Q factors that range from 8 to 20, while for the parabolic ones the Q factors lie in the range 40 to 80. The improved Q factor and well-defined resonance enables frequency selectivity. It is possible to conceive of a nonvolatile memory or logic system where binary data are stored as the absence or presence of a domain wall in a series of pinning potentials along a nanowire, each engineered through lithography to have a different eigenfrequency. No external or variable magnetic fields, which are costly to generate in terms of energy, would be needed to control the eigenfrequency, as was the case in the design presented in Ref. 6. DWs in an array of such notches could then be individually addressed and manipulated, e.g., through resonantly assisted depinning,[14,24] without requiring individual contacts for each notch, significantly reducing the complexity of the wiring needed to control such a memory.

This research was supported by the ESF EUROCORES collaborative research project SpinCurrent under the Fundamentals of Nanoelectronics program, and by the EPSRC-GB through the Spin@RT consortium. We are grateful to the Diamond Light Source for the provision of beamtime.

*s.lepadatu@leeds.ac.uk
†c.h.marrows@leeds.ac.uk

[1] L. Berger, J. Appl. Phys. **55**, 1954 (1984).
[2] Z. Li and S. Zhang, Phys. Rev. B **70**, 024417 (2004).
[3] I. Žutić *et al.*, Rev. Mod. Phys. **76**, 323 (2004).
[4] S. S. P. Parkin *et al.*, Science **320**, 190 (2008).
[5] P. Xu *et al.*, Nat. Nanotechnol. **3**, 97 (2008).
[6] E. Saitoh *et al.*, Nature (London) **432**, 203 (2004).
[7] G. Tatara *et al.*, Appl. Phys. Lett. **86**, 232504 (2005).
[8] N. L. Schryer and L. R. Walker, J. Appl. Phys. **45**, 5406 (1974).
[9] S. Lepadatu *et al.*, Phys. Rev. B **79**, 094402 (2009).
[10] S. Lepadatu *et al.*, Phys. Rev. Lett. **102**, 127203 (2009).
[11] C. H. Marrows, Adv. Phys. **54**, 585 (2005).
[12] L. Thomas *et al.*, Nature (London) **443**, 197 (2006).
[13] E. Martinez *et al.*, Phys. Rev. B **77**, 144417 (2008).
[14] E. Martinez *et al.*, Phys. Rev. B **79**, 094430 (2009).
[15] J. Stöhr *et al.*, Science **259**, 658 (1993).
[16] R. Allenspach, J. Magn. Magn. Mater. **129**, 160 (1994).
[17] R. D. McMichael and M. J. Donahue, IEEE Trans. Magn. **33**, 4167 (1997).
[18] A. P. Malozemoff and J. C. Slonczewski, *Magnetic Domain Walls in Bubble Materials* (Academic, New York, 1979).
[19] J. A. Osborn, Phys. Rev. **67**, 351 (1945).
[20] G. Tatara and H. Kohno, Phys. Rev. Lett. **92**, 086601 (2004).
[21] A. Thiaville *et al.*, J. Appl. Phys. **95**, 7049 (2004).
[22] P. Bruno, Phys. Rev. Lett. **83**, 2425 (1999).
[23] G. Tatara *et al.*, Phys. Rep. **468**, 213 (2008).
[24] D. Bedau *et al.*, Phys. Rev. Lett. **99**, 146601 (2007).
[25] D. Bedau *et al.*, Phys. Rev. Lett. **101**, 256602 (2008).
[26] Y. Nakatani *et al.*, Nature Mater. **2**, 521 (2003).
[27] J. O. Rantschler, IEEE Trans. Magn. **41**, 3523 (2005).